# Implementation and Validation of a Lumped Model for an Experimental Multi-Span Web Transport System

# Implementation and validation of a lumped model for an experimental multi-span web transport system

N.I. Giannoccaro[1], G. Manieri[2], P. Martina[3] and T. Sakamoto[4]

***Abstract*— Correct modeling is necessary in order to design a better control system or to identify the plant parameters experimentally. On the web dynamics itself, lumped parameters expressions may be used to designate a web section between two adjacent drive rolls, and there is the necessity of incorporating the property of viscoelasticity to the web. Lumped model of an experimental multi-span web transport system is based on the conservation mass, torque balance and viscoelasticity. A new way for describing this kind of MIMO system has been introduced through a four by four *Transfer Matrix* which considers mutual interactions between inputs and outputs. Finally, comparing experimental data with Transfer Matrix parametric expressions, it has been possible to identify the system parameters and thus fully validate the effectiveness of the proposed dynamic lumped model.**

## I. INTRODUCTION

Wet paper or polymeric film exhibit viscoelastic characteristic which may be expressed in terms of Maxwell element, Voigt element or other viscoelastic elements as first suggested by T.Sakamoto in 1995 [1]. By introducing these viscoelastic models it has been possible to implement and improve decentralized robust control strategies like smart decomposition of the system (*Overlapping decomposition* [2]) and more complex control strategies like *H∞ control* [3] and *Neuro Fuzzy control* [4]. Lumped model, which will be presented in this paper, is referred to an experimental system [5], [6], [7] consisting of four sections: an unwinder section, a leading section, a draw roll section and a winder section, each one driven by one servomotor. A web transport system has a structure of multi-inputs and multi-outputs (MIMO), which consists of many subsystems with strong interactions between neighboring subsystems through the associated web tensions. These subsystems are divided into two main groups of systems such as tension control and speed control systems. In this paper a new strategy for system parameters identification is proposed. It is based on the definition of a four-by-four *Transfer Matrix* which made possible to fully validate a lumped dynamic model of the web handling system.

## II. EXPERIMENTAL WEB HANDLING SYSTEM

### A. Description of the apparatus

The realized system, already introduced in [8], [9] consists of four main sections strongly interlaced each other and 12 rolls placed on a mechanical frame at different heights. The system has been completely renewed at the end of 2015, substituting all the rolls and their bearings with new ones with high performances (low weight and low friction). The transport system is driven by 4 servomotors (750 $[W]$, 2,39 $[N\,m]$), one for each subsystem, and divide the whole system in three spans having length respectively named $L_1$, $L_2$ and $L_3$. In Fig.1 are depicted web tensions, $T_k$, the input torque signals, $u_k$, and the system geometric characteristic, $r_k$ and $J_k$, respectively rollers radius and inertia. Two couples of

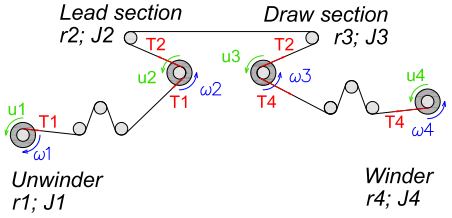


Fig. 1: Dynamic scheme

tension sensors (one for each side of the web) are placed on the corresponding locations. The first couple of sensors is placed after the unwinder roll and the second one right before the winder roll. All servomotors are set in torque control mode. In particular, the voltage input signals $U_i$, $i = 1,\ldots,4$, are sent to the servomotors thus producing the torque input, $u_k$, by using a 4 channels D/A board. The tension sensor signals feed the A/D board and the average value of the two corresponding sides is considered for measuring the tension after the unwinder (named $T_1$) and before the winder (named $T_4$). The 4 motor encoder signals (including the speed signals of unwinder section and winder section) feed a digital counter: in the proposed identification strategy the velocity of the lead section (named $v_2$) and of the draw-roll section (named $v_3$). The controller's CPU receives signals through A/D boards and counters, performs the control algorithm (C language and Linux OS) and outputs the command signals in real time to the motor driver via D/A boards with a sampling time of 0.01 $[s]$.

### B. Geometric system specifications

Rollers inertia has been already identified [9] with respect to both lead section and draw section rollers, assuming that their values were the same and constant while transporting the web. Unwinder and winder rollers inertia are then given by the sum of the constant identified term of the unloaded rollers ($J = 0.0011\,[kgm^2]$) and the term due to the wrapped

[1], [2] and [3] are with Department of Innovation Engineering, University of Salento, Lecce, Italy. Email: ivan.giannoccaro@unisalento.it; Tel. +390832297813

[4] is with Department of Control Engineering, Kyushu Institute of Technology, Tobata, Kitakyushu, Japan. Email: sakamoto@cntl.kyutech.ac.jp

web on it considered as an hollow cylinder. Two additional inertial terms, $J_a = 0.003\ [kg\,m^2]$ and $J_b = 0.005\ [kg\,m^2]$, have been added in order to better match transient state system behavior with trial-and-error approach.

$$J_1 = J + \frac{1}{2}\rho\,\pi\,(r_1^4 - r_2^4)\,w + J_a \tag{1}$$

$$J_2 = J + J_b$$

$$J_3 = J + J_b$$

$$J_4 = J + \frac{1}{2}\rho\,\pi\,(r_4^4 - r_2^4)\,w + J_a$$

This model doesn't keep into account the problem of winder and unwinder external radii variation and assumes that their inertia remain constant during web transportation, as well. These hypothesis are reasonably accepted in case of low web speed transfer and short in time winding processes. Geometric and mass properties of the 4 drive rolls are shown in Tab.I.

TABLE I: Geometric properties of the platform

| Section | Symbol | Value |
|---|---|---|
| UNWINDER | | |
| Radius | $r_1$ | $3.26 \cdot 10^{-2}$ $[m]$ |
| Inertia | $J_1$ | $4.42 \cdot 10^{-3}$ $[kg\,m^2]$ |
| Span | $L_1$ | 0.75 $[m]$ |
| LEADING | | |
| Radius | $r_2$ | $2.5 \cdot 10^{-2}$ $[m]$ |
| Inertia | $J_2$ | $6.1 \cdot 10^{-3}$ $[kg\,m^2]$ |
| Span | $L_2$ | 1.2 $[m]$ |
| DRAW ROLL | | |
| Radius | $r_3$ | $2.5 \cdot 10^{-2}$ $[m]$ |
| Inertia | $J_3$ | $6.1 \cdot 10^{-3}$ $[kg\,m^2]$ |
| Span | $L_3$ | 1.25 $[m]$ |
| WINDER | | |
| Radius | $r_4$ | $3.22 \cdot 10^{-2}$ $[m]$ |
| Inertia | $J_4$ | $4.39 \cdot 10^{-3}$ $[kg\,m^2]$ |

At an elementar level, between the many web material properties that could be measured, those that most influence web handling include Young's modulus, strength (ultimate stress and strain), basis weight, thickness and friction coefficients. The immediate application of strength is to determine appropriate tension set-point ranges. There is a convenient rule of thumb that says many webs will handle best when tensioned between 10% and 25% of their strength. The following table (Tab.II) sums up the main material properties about the OPP film used in the experimental web handling system.

## III. Lumped model for the experimental web transport system

### A. Modeling of the system

The modeling of the web transport system is based on three laws [9], [1] applied at each section between two consecutive rolls and usually written in the Laplace domain:

TABLE II: Phisycal properties of the OPP film

| Unwinder section | Symbol | Value |
|---|---|---|
| Width | w | 0.3 $[m]$ |
| Thickness | Th | $4 \cdot 10^{-5}$ $[m]$ |
| Cross-sectional area | A | $1.2 \cdot 10^{-5}$ $[m^2]$ |
| Density | $\rho$ | 910 $[kg/m^3]$ |
| Young's modulus | E | $9.8 \cdot 10^{9}$ $[N/m^2]$ |
| Tensile strength | $\sigma_R$ | $32 \cdot 10^{6}$ $[N/m^2]$ |
| Yield strength | $\sigma_Y$ | $22 \cdot 10^{6}$ $[N/m^2]$ |
| Viscosity coefficient | $\eta$ | $1.5 \cdot 10^{9}$ $[Ns/m^2]$ |

a) **Mass conservation**

$$\varepsilon(s) = \frac{1}{L_j\,s}\left[v_b(s) - v_a(s)\right] \tag{2}$$

b) **Torque balance**

$$\begin{aligned} s\,J_k\,\omega_k = {} & r_k\,(T_{k+1}(s) - T_k(s)) + u_k(s) \\ & - C_k(s) - k_{fk}\,\omega_k(s) \end{aligned} \tag{3}$$

c) **Voigt viscoelastic model**

$$T_k(s) = A\,\eta\,\frac{1 + T_v(s)}{T_v(s)}\,s\,\varepsilon(s) \tag{4}$$

where $T_v = \frac{\eta}{E}$.

Assuming that the web does not completely slide on the roll, the velocity is considered equal to the roll linear velocity. The angular velocity $\omega_k$ of the $k^{th}$ roll can be obtained through a torque balance in function of the tension forces $T_{k+1}$ and $T_k$ applied to the roll from the web (3). $u_k$ is the motor torque applied to the $k^{th}$ roll which is proportional to the motor voltage control signal, $U_k$, by means of the motor constant $K_k$ ($u_k(t) = K_k U_k(t)$), $C_k$ is the dry friction torque, which value is time-depending until steady state is reached and finally $k_{fk}$ is the viscous friction coefficient. The possibility of using algebraic equations in (2), (3), (4) in the Laplace domain gives the possibility of building in simple way a block diagram of the entire system considering the equation related to the different system sections. In this case the unwinder section, the leading section, the draw-roll section and the winder section are respectively numbered with 1, 2, 3 and 4. System outputs are represented by $T_1$ and $T_4$ tensions and by the longitudinal speed of the rolls of the sections 2 and 3, $v_2$ and $v_3$.

### B. Dynamic block diagram

Starting from (3) and referring to the dynamic scheme in Fig.1 it is possible to write torque balance for each subsystem. Using the four torque balance equations it is possible to calculate the peripheral speeds of the web for each subsystem ($\omega_k = \frac{v_k}{r_k}$). Block diagrams may be easily developed in the Laplace domain using the block system algebra in order to explicit the algebraic equations and find the values of $v_1$, $v_2$, $v_3$, $v_4$ as it is shown as example for the unwinder block in Fig3. According to (2), mass conservation

can be applied and, eventually, Voigt-Kelvin viscoelasticity law (4) allows to determine the values of $T_1$, $T_2$, and $T_4$.

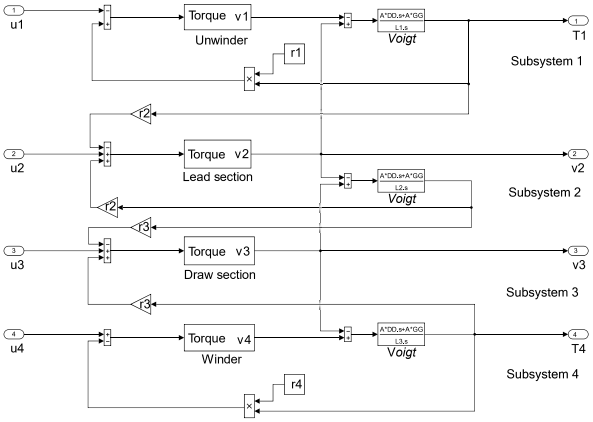


Fig. 2: Dynamic block diagram

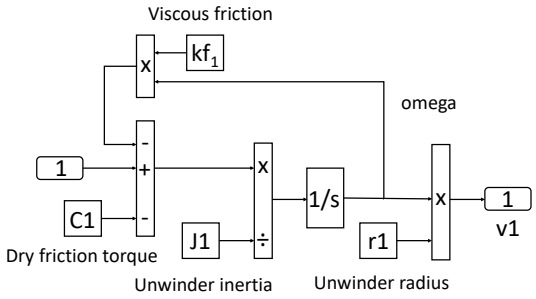


Fig. 3: Torque balance for the unwinder block

The dynamic block diagram shown in Fig2 is graphically significant about the interactions of the different subsystems that form the full system model. However, at the same time, it shows its inner limits in case of studying the dependence of each output from one single input. At the moment, many issues affect the dynamic model. First of all the problem that concerns system parameters identification such as steady-state dry friction torque, $C_k$, and viscous friction, $k_{fk}$. Moreover it would be academically interesting finding a way for expressing each system responses ($T_1$, $v_2$, $v_3$, $T_4$) by means of all system inputs. This requires the definition of a 4 by 4 **Transfer Matrix**, which elements are represented by 16 transfer functions. This paper proposes a brand new solution to these problems and a new approach of studying MIMO systems through the definition of a Transfer Matrix.

## IV. System parameters identification

### A. Calculation strategy

MIMO systems need a peculiar way of describing system dynamics. The most effective is managing (2), (3), (4) and apply them at each subsystem until obtaining the dependency of each output, $T_1$, $v_2$, $v_3$, $T_4$, from all of the four inputs, $u_1$, $u_2$, $u_3$, $u_4$. This leads to the definition of a 4 by 4 **Transfer Matrix** where each one of the sixteen terms is represented by a transfer function in Laplace domain. Because of the presence of recurrent terms, it is convenient declaring the following statements:

$$\alpha = \delta = sJ_2 + k_{f2}$$
$$\beta = sJ_1 + k_{f1}$$
$$\gamma = \mu = sJ_3 + k_{f3}$$
$$\lambda = sJ_4 + k_{f4}$$
$$\chi_1 = \frac{P}{L_1\alpha\beta + Pr_2^2\beta + Pr_1^2\alpha}$$
$$\chi_2 = \frac{P}{L_2\gamma\delta + Pr_3^2\delta + Pr_2^2\gamma}$$
$$\chi_4 = \frac{P}{L_3\lambda\mu + Pr_4^2\mu + r_3^2\lambda P}$$

The following (5), (6), (7) represent the simplified expressions of the outputs $T_1$, $T_4$ and of the tension $T_2$, necessary for calculating the outputs $v_2$ and $v_3$.

$$\begin{aligned} T_1 = {} & u_1(a_1 r_1 \alpha) + u_2(a_1 r_2 \beta - a_1 b_1 r_2^3 \beta\gamma) \\ & + u_3(a_1 b_1 r_2^2 \beta r_3 \delta - a_1 b_1 r_2^2 \beta \chi_4 r_3^3 \delta\lambda) \\ & + u_4(a_1 b_1 r_2^2 \beta \chi_4 r_3^2 \delta r_4 \mu) \\ & + (-a_1 b_1 r_2^2 \beta \chi_4 r_3^2 \delta C_4 r_4 \mu \\ & + a_1 b_1 r_2^2 \beta \chi_4 r_3^3 \delta C_3 \lambda \\ & - a_1 b_1 r_2^2 \beta C_3 r_3 \delta + a_1 b_1 r_2^3 \beta C_2 \gamma \\ & - a_1 C_2 r_2 \beta + a_1 C_1 r_1 \alpha) \end{aligned} \quad (5)$$

Where in (5):

$$a_1 = \frac{\chi_1}{1 - \frac{r_2^4 \gamma \chi_1 \chi_2 \beta}{1 - \chi_2 \chi_4 r_3^4 \lambda \delta}}$$
$$b_1 = \frac{\chi_2}{1 - \chi_2 \chi_4 r_3^4 \lambda \delta}$$

$$\begin{aligned} T_4 = {} & u_1(a_4 b_4 r_3^2 \lambda \chi_1 r_2^2 \gamma r_1 \alpha) \\ & + u_2(a_4 b_4 r_3^2 \lambda \chi_1 r_2^3 \gamma\beta - a_4 b_4 r_3^2 \lambda r_2 \gamma) \\ & + u_3(a_4 b_4 r_3^3 \lambda \delta - a_4 r_3 \lambda) + u_4(a_4 r_4 \mu) \\ & + (-a_4 C_4 r_4 \mu - a_4 b_4 r_3^3 \lambda C_3 \delta \\ & - a_4 b_4 r_3^3 \lambda \chi_1 C_2 r_2^3 \gamma\beta \\ & + a_4 b_4 r_3^2 \lambda r_2^2 \gamma r_1 C_1 \alpha \chi_1 \\ & + a_4 b_4 r_3^2 \lambda C_2 r_2 \gamma + a_4 C_3 r_3 \lambda) \end{aligned} \quad (6)$$

Where in (6):

$$a_4 = \frac{\chi_4}{1 - \frac{\chi_2 \chi_4 r_3^4 \delta \lambda}{1 - \chi_1 \chi_2 r_2^4 \beta \gamma}}$$
$$b_4 = \frac{\chi_2}{1 - \chi_1 \chi_2 r_2^4 \beta \gamma}$$

$$\begin{aligned} T_2 = {} & u_1(f \chi_1 r_2^2 \gamma r_1 \alpha) + u_2(f \chi_1 r_2^3 \gamma\beta - f r_2 \gamma) \\ & + u_3(f r_3 \delta - f \chi_4 r_3^2 \delta r_4 \mu) \\ & + u_4(f \chi_4 r_3^2 \delta r_4 \mu) \\ & + (-f \chi_4 r_3^3 \delta C_4 r_4 \mu + f \chi_4 r_3^3 \delta C_3 \lambda - f C_3 r_3 \delta \\ & - f \chi_1 r_2^3 \gamma C_2 \beta + f \chi_1 r_2^2 \gamma C_1 r_1 \alpha + f C_2 r_2 \gamma) \end{aligned} \quad (7)$$

Where in (7):

$$f = \frac{\chi_2}{1 - \chi_2 \chi_4 r_3^4 \delta \lambda - \chi_1 \chi_2 r_2^4 \gamma \beta}$$

Only now it's possible to extract an output expression of $v_2$ and $v_3$ depending exclusively on the four inputs $u_1$, $u_2$, $u_3$ and $u_4$.

$$\begin{aligned} v_2 = \frac{1}{\alpha} [ & u_1 (f r_2^4 \chi_1 \gamma r_1 \alpha - a_1 r_2^2 r_1 \alpha) \\ & + u_2 (r_2 - a_1 r_2^3 \beta + a_1 b_1 r_2^5 \beta \gamma + f \chi_1 r_2^5 \gamma \beta - f r_2^3 \gamma) \\ & + u_3 (f r_2^2 r_3 \delta - f r_2^2 \chi_4 r_3^3 \delta \lambda - a_1 b_1 r_2^4 \beta r_3 \delta \\ & + a_1 b_1 r_2^4 \beta \chi_4 r_3^3 \delta \lambda) \\ & + u_4 (f r_2^2 \chi_4 r_3^2 \delta r_4 \mu - a_1 b_1 r_2^4 \beta \chi_4 r_3^2 \delta r_4 \mu) \\ & + (a_1 b_1 r_2^4 \beta \chi_4 r_3^2 \delta C_4 r_4 \mu \\ & - a_1 b_1 r_2^4 \beta \chi_4 r_3^3 \delta C_3 \lambda + a_1 b_1 r_2^4 \beta C_3 r_3 \delta \\ & - a_1 b_1 r_2^5 \beta C_2 \gamma + a_1 C_1 r_1 r_2^2 \alpha \\ & - f r_2^2 \chi_4 r_3^2 \delta C_4 r_4 \mu + f r_2^2 r_3^3 \chi_4 \delta C_3 \lambda \\ & - f r_2^5 \chi_1 \gamma C_2 \beta + f r_2^4 \gamma \chi_1 C_1 r_1 \alpha \\ & + f r_2^3 \gamma C_2 - C_2 r_2)] \end{aligned} \tag{8}$$

$$\begin{aligned} v_3 = \frac{1}{\gamma} [ & u_1 (a_4 b_4 r_3^4 \lambda \chi_1 r_2^2 \gamma r_1 \alpha - f r_3^2 \chi_1 r_2^2 \gamma r_1 \alpha) \\ & + u_2 (a_4 b_4 r_3^4 \lambda \chi_1 r_2^3 \gamma \beta - a_4 b_4 r_3^4 \lambda r_2 \gamma \\ & - f \chi_1 r_2^3 r_3^2 \gamma \beta + f r_3^2 r_2 \gamma) \\ & + u_3 (r_3 + a_4 b_4 r_3^5 \lambda \delta - a_4 r_3^3 \lambda \\ & - f r_3^3 \delta + f r_3^5 \delta \lambda \chi_4) \\ & + u_4 (a_4 r_3^2 r_4 \mu - \chi_4 f r_3^4 \delta r_4 \mu) \\ & + (\chi_4 f r_3^4 \delta C_4 r_4 \mu - f \chi_4 r_3^5 \delta C_3 \lambda + f C_3 r_3^3 \delta \\ & + f \chi_1 r_2^3 r_3^2 \gamma C_2 \beta \\ & - f \chi_1 r_2^3 r_3^2 \gamma C_1 r_1 \alpha - f r_3^2 C_2 r_2 \gamma - a_4 r_3^2 C_4 r_4 \mu \\ & - a_4 b_4 r_3^5 \lambda C_3 \delta - a_4 b_4 r_3^4 \lambda \chi_1 C_2 r_2^3 \gamma \beta \\ & + a_4 b_4 r_3^4 \lambda r_2^2 \gamma r_1 C_1 \alpha \chi_1 \\ & + a_4 b_4 r_3^4 \lambda C_2 r_2 \gamma + a_4 C_3 r_3^3 \lambda - C_3 r_3)] \end{aligned} \tag{9}$$

### B. Transfer Matrix

Output expressions (5), (6), (8) and (9) show a direct dependency on input signals $u_1$, $u_2$, $u_3$ and $u_4$ by means of transfer functions which can be organized in the shape of a **Transfer Matrix**: $\{y\} = [H]\{u\} + \{d\}$.

$$\begin{Bmatrix} T_1 \\ v_2 \\ v_3 \\ T_4 \end{Bmatrix} = \begin{bmatrix} H_{11} & H_{12} & H_{13} & H_{14} \\ H_{21} & H_{22} & H_{23} & H_{24} \\ H_{31} & H_{32} & H_{33} & H_{34} \\ H_{41} & H_{42} & H_{43} & H_{44} \end{bmatrix} \begin{Bmatrix} u_1 \\ u_2 \\ u_3 \\ u_4 \end{Bmatrix} + \begin{Bmatrix} d_1 \\ d_2 \\ d_3 \\ d_4 \end{Bmatrix} \tag{10}$$

Where:

- $\{y\}$ is the outputs vector;
- $\{u\}$ is the inputs vector;
- $\{d\}$ is the constant terms vector;
- $[H]$ is Transfer Matrix.

Transfer matrix approach represents an alternative way of expressing the same system dynamics, already introduced with block diagram (Fig.2), but with the advantage of separating the effects on each output due to each signal input $u_k$. Most important consequence is that each transfer function is parameterized on $k_{fk}$ and $C_k$ coefficients. In particular, $H_{ij}$ transfer functions depend only on viscous friction coefficients, $k_{fk}$; $d_i$ terms in (10), instead, depend on both dry friction torque, $C_k$, and viscous friction coefficients, $k_{fk}$. That means that an optimization strategy for system parameters identification can be carried on by using scientific commercial software.

### C. System parameter identification strategy

According to Koç [10], a valid approach to system parameters identification is based on *Model Matching Method*. A similar optimization method is presented in this paper. This method focuses on obtaining steady state expressions from transfer functions and minimizing the error function between the steady state Transfer Matrix dynamic model and the single step system output response data gathered from open loop experimental tests. Model matching method needs preliminary to collect data from experimental tests which have been carried out without feedback control. The following sets of voltage input, named A, B, C and D have been chosen and assigned respectively to unwinder, lead-section, draw-roll and winder servomotors. As example, experimental data of Test A are shown in Fig.4.

- A: [0.35 0.08 0.08 0.5];
- B: [0.2 0.06 0.06 0.4];
- C: [0.2 0.08 0.08 0.3];
- D: [0.3 0.08 0.08 0.4];
- E: [0.4 0.08 0.08 0.55];

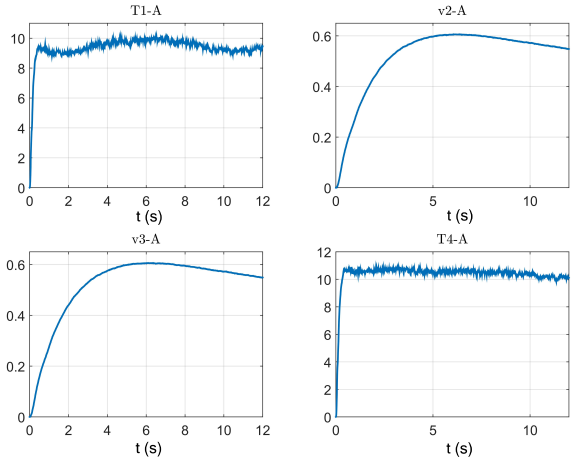


Fig. 4: Test A experimental data

### D. $C_k$ and $k_{fk}$ effect on the system outputs

Before introducing the problem of optimization, it would be of interest to deepen the effects that both steady-state dry friction torque, $C_k$, and $k_{fk}$ coefficient have on the

dynamic behavior of the system and may discover some interesting properties useful to simplify calculations. In this regard system parameters identification would be necessary. In first approximation, it is sufficient to consider viscous friction coefficients and dry friction torques identified [9] for a preview version of the same web tension system. It is very important pointing out that these values refers to very different working conditions compared to the actual system, both from the structural point of view (different sizes of servomotors) and from the set point specifications point of view (Tension and web speed). This is why new identification is needed. However it is reasonable to accept, at least in terms of magnitude, the following values:

- $C_{k,id}$: [0.00372 0.04513 0.00012 0.00010];
- $k_{fk,id}$: [0.03869 0.02817 0.05119 0.00089].

Figure 5 shows what happens when $C_k = 0$ and the rest of the system is parameterized on the $k_{fk}$ factors. Opportunely changing multiplicative factors, $T_1$ and $T_4$ are described quite well; web speeds, $v_2$ and $v_3$ show a remarkable shift up and down with respect to $k_{fk} = 1\,k_{fk,id}$ curve, whether multiplicative factor is, respectively, lower and greater than 1. The most important consequence to what has just been discovered is that it is possible to simplify the definition of Transfer Matrix, neglecting the vector of coefficients $\{d\}$ in (10). In fact, whether $H_{ij}$ transfer functions depend only on viscous coefficients, $d_{i1}$ terms depend on both $k_{fk}$ and $C_k$ coefficients, and as $C_k$ contribution is negligible, then also the respective $d_{i1}$ values are negligible as well. (10) can be rewritten as follows:

$$\{y\} = [H]\{u\} \tag{11}$$

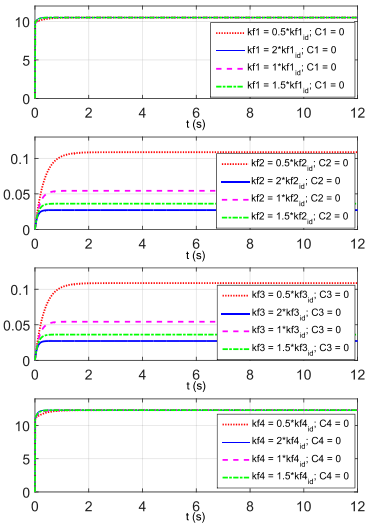


Fig. 5: Variable $k_{fk}$, $C_k = 0$

## E. Steady state Transfer Matrix

Output average values have been obtained starting from $t = 6\,[s]$ in order to avoid any influence due to transient state and will represent the upper reference limits for the optimization algorithm. In this regard Transfer Matrix elements, $H_{ij}$, need to be manipulated until steady state expressions of the original transfer functions are obtained. A convenient strategy is neglecting Laplace variable depending terms and considering the only contributions due to constant terms. As already mentioned above, each transfer function, $H_{ij}$, is obtained as ratio of two polynomials:

$$H_{ij} = \frac{a_1 + a_2 s + \cdots + a_k s^{k-1} + \cdots + a_m s^{m-1}}{b_1 + b_2 s + \cdots + b_l s^{l-1} + \cdots + b_n s^{n-1}}$$

$$k = 1, \ldots, m; \qquad l = 1, \ldots, n; \qquad m \leq n$$

Neglecting any time depending contribution means considering the only constant terms $a_1$ and $b_1$. Transfer function can be rewritten as follows:

$$H^*_{ij} = \frac{a_1(k_{fk})}{b_1(k_{fk})}$$

Where $a_1$ and $b_1$ are functions of viscous frictions $k_{fk}$ which values are still unknown and will be object of the next optimization procedure.

## F. Optimization

Optimization algorithm usually need a cost function. As it's been shown above, cost functions will include two main information. First one is the average steady state response value of the system outputs: $\overline{\overline{T_1}}$, $\overline{\overline{v_2}}$, $\overline{\overline{v_3}}$ and $\overline{\overline{T_4}}$; second one is a parametric function, here represented by steady state transfer function polynomials. Cost functions can be written as follows:

$$f_1(k_{fk}) = |\overline{\overline{T_1}} - (u_1 H^*_{11} + u_2 H^*_{12} + u_3 H^*_{13} + u_4 H^*_{14})| \tag{12}$$

$$f_2(k_{fk}) = |\overline{\overline{v_2}} - (u_1 H^*_{21} + u_2 H^*_{22} + u_3 H^*_{23} + u_4 H^*_{24})| \tag{13}$$

$$f_3(k_{fk}) = |\overline{\overline{v_3}} - (u_1 H^*_{31} + u_2 H^*_{32} + u_3 H^*_{33} + u_4 H^*_{34})| \tag{14}$$

$$f_4(k_{fk}) = |\overline{\overline{T_4}} - (u_1 H^*_{41} + u_2 H^*_{42} + u_3 H^*_{43} + u_4 H^*_{44})| \tag{15}$$

Optimization has been carried out with *FMinMax* algorithm. Taking example from preview studies on the same web transport system, it has been imposed that $k_{fk}$ values should belong to a range between 0.001 and 1. Table III shows all the identified $k_{fk}$ values coming from the optimization routine. Before accepting these values it is necessary to verify

TABLE III: Identified $k_{fk}$ values

| Test | $k_{f1}\,[kg\,m^2/s]$ | $k_{f2}\,[kg\,m^2/s]$ | $k_{f3}\,[kg\,m^2/s]$ | $k_{f4}\,[kg\,m^2/s]$ |
|---|---|---|---|---|
| A | 0.0016 | 0.0030 | 0.0030 | 0.0034 |
| B | 0.0015 | 0.0023 | 0.0023 | 0.0031 |
| C | 0.0024 | 0.0049 | 0.0048 | 0.0056 |
| D | 0.0030 | 0.0055 | 0.0053 | 0.0061 |
| E | 0.0013 | 0.0038 | 0.0046 | 0.0052 |

if they fit well the experimental data. Most important is first demonstrating that, through the identified $k_{fk}$ values, *Dynamic Model* and *Transfer Matrix Model* behave at the same way; next the problem of validation will be addressed.

## V. Model validation with identified $k_{fk}$ values

With identification is now possible to compare both Dynamic and Transfer Matrix models and verify that they perfectly match and above all, depending on the $k_{fk}$ identified values, both of them fit experimental data (Figs.6, 7, 8).

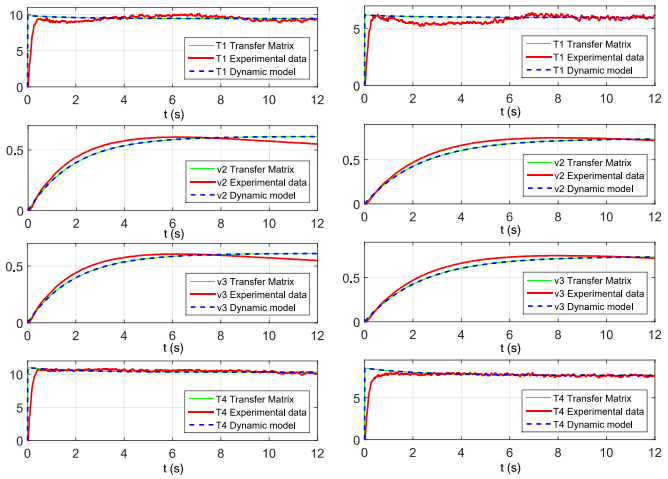


(a) *Test A - Validation* (b) *Test B - Validation*

Fig. 6: Test A - Test B Validation

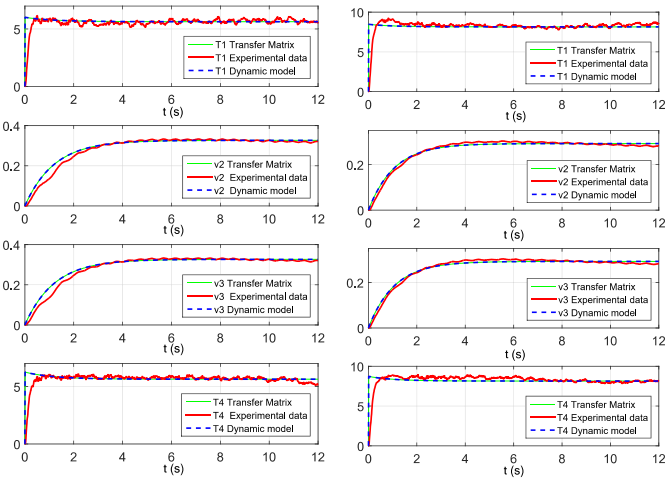


(a) *Test C - Validation* (b) *Test D - Validation*

Fig. 7: Test C - Test D Validation

## VI. Conclusions

A simpler and more effective approach for MIMO system parameters identification is shown. It consists in representing the system dynamics through a $n$ x $n$ Transfer Matrix that directly and selectively links inputs to outputs. Moreover this strategy allows to write transfer functions parameterized on the unknown values of $k_{fk}$ and $C_k$, thus introducing a great advantage in finding these values through an optimization routine. A long experimental campaign provided open loop data on the system output behavior. Optimization consists

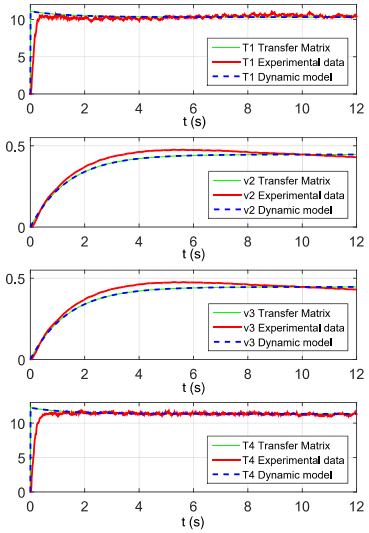


Fig. 8: Test E - Validation

in minimizing a convenient cost function represented by the difference between steady state system output response and the parameterized expression of the steady state transfer functions. *FMinMax* optimization routine could find the set of viscous friction coefficients for all the different working conditions of the bench machine. The validated dynamic model is also useful for further involvements about the design of an effective PI controller [11].

## References


[1] T. Sakamoto, Y. Fujino. *"Modelling and analysis of a web tension control system"* in Proc. IEEE Int. Symp. on Industrial Electronics, 1995, pp.358-362.

[2] T. Sakamoto. *"PI control of web tension control system based on overlapping decomposition"* in IEEE Nordic Workshop on Power and Industrial Electronics, 1998, pp.158-163.

[3] N. I. Giannoccaro, T. Nishida and T. Sakamoto. *"Decentralized Control Performances of an Experimental Web Handling System"* in International Journal of Advanced Robotic Systems, 2012, pp.141.

[4] N. I. Giannoccaro, I. Uchitomi and T. Sakamoto. *"Decentralized Neuro-Fuzzy Control of an Experimental Web Transport Platform"*

[5] N. I. Giannoccaro, K. Oishi and T. Sakamoto. *"An experimental web tension control system: system set-up"* in Advances in Production Engineering and Management, 2007, pp.185-193.

[6] N. I. Giannoccaro and T. Sakamoto. *"Analysis of a complex experimental web tension control system"* in Proceedings of the 18th Aimeta Conference, 2007.

[7] N. I. Giannoccaro and T. Sakamoto. *"Development of a new experimental web tension control system"* in DAAM International Scientific Book, 2008, pp.301-316.

[8] N. I. Giannoccaro, T. Sakamoto and I. Uchitomi. *"Performance of a web transport system with tension control subsystem using speed as control input"* in IEEE Industrial Electronic Society, 2015, pp.1-6.

[9] N. I. Giannoccaro, A. Messina and T. Sakamoto. *"Updating of a lumped model for an experimental web tension control system using a multivariable optimization method"* in Applied Mathematical Modelling, 2010, pp. 671-683.

[10] H. Koç, D. Knittel, M. De Mathelin and G. Abba. *"Modeling and Robust Control of Winding Systems for Elastic Webs"* in IEEE Transactions on control systems technology, 2002.

[11] N. I. Giannoccaro, G. Manieri, P. Martina, T. Sakamoto. *"Genetic algorithm for decentralized PI controller tuning of a multi-span web transport system based on overlapping decomposition"*. In Australian and New Zealand Control Conference - ANZCC 2017, Gold Coast,17-20 December 2017.